Synthesis of Silver Nanoparticles in Electrospun Polyacrylonitrile Nanofibers Using Tea Polyphenols as the Reductant

MeiLing Zou,[1] MingLiang Du,[1,2] Han Zhu,[1] CongSheng Xu,[1] Ni Li,[1,2] YaQin Fu[1,2]
[1] *Department of Materials Engineering, College of Materials and Textile, Zhejiang Sci-Tech University, Hangzhou 310018, People's Republic of China*

[2] *Key Laboratory of Advanced Textile Materials and Manufacturing Technology, Zhejiang Sci-Tech University, Ministry of Education, Hangzhou 310018, People's Republic of China*

Uniformly dispersed Ag nanoparticles (AgNPs) with diameter about 5 nm embedded in electrospun polyacrylonitrile (PAN) nanofibers were synthesized by using tea polyphenols (TP) as the reductant. The reducing ability of TP toward Ag ions was characterized by Fourier transform infrared spectroscopy and ultraviolet–visible spectra, and the results revealed that TP exhibit satisfied reducing ability in the synthesis process. Transmission electron microscopy observation showed that the synthesized spherical AgNPs with diameter about 5 nm were immobilized on the surface and in the interior of PAN nanofibers by electrospinning technology. The interactions of Ag with PAN and TP were investigated by X-ray photoelectron spectroscopy (XPS), and the results suggested that PAN polymer and TP both served as stabilizer during the synthesis of AgNPs because of the chelating interactions of Ag with cyano groups and phenolic hydroxyls. The synthesized AgNPs in PAN nanofibers exhibit good antibacterial property and may be used for antibacterial and catalytic applications. **POLYM. ENG. SCI., 53:1099–1108, 2013.**

INTRODUCTION

Ag nanoparticles (AgNPs) have deserved special attention owing to their fascinating physical and chemical properties [1–4] and, so far, diverse applications of AgNPs have been explored in chemical, catalytic, biological, and other fields [5–8]. Typically, AgNPs present high reactivity and selectivity in a broad range of catalytic reactions. As reported, Shen et al. developed highly monodispersed Cu- and Ag-based bimetallic nanocrystals for the efficient catalyst of CO oxidation [5]. Besides, AgNPs possess strong antimicrobial properties against various species of bacteria, low toxicity to human beings, and a long-term antibacterial efficiency, now that they have been applied in many related fields, such as pharmaceutical, silver-coated medical devices, textiles, food packaging, and so on [9–12].

It is well recognized that the size, shape, and surface properties of AgNPs are closely related to their properties; however, smaller AgNPs are easy to aggregate due to their high surface energy, so synthesis of AgNPs with small size and uniform dispersion has been devoted great efforts in recent years. During the application of AgNPs, they are often fastened to organic polymer or inorganic support to avoid aggregation [13–16]. Guo et al. have done much work on the synthesis of small and size-controlled AgNPs using tannin-grafted collagen fiber [6]. Jean et al. reported the synthesis of functionalized silica nanoparticles decorated by nanometallic Ag for optical sensing [1]. However, it should be mentioned that traditional chemical reductants, such as $NaBH_4$, dimethylhydrazine, hydrazine, and so forth, are environmental intolerance and will bring potential environment risk. Some green reducing agents have been reported to synthesize metallic nanoparticles, such as gold, platinum, and iron [17–19]. Consequently, it is meaningful to explore a facile approach for the synthesis of uniformly dispersed AgNPs with small particle size.

Plant polyphenols pervasively exist in the plant kingdom, like vegetables, fruits, beverages, and tea [20, 21]. Tea polyphenols (TP) are extracted from tea plants, and they are mixtures of polyphenol compounds belonging to the flavonoid family, mainly including catechin (EC),

Correspondence to: MingLiang Du; e-mail: du@zstu.edu.cn
Contract grant sponsor: National Natural Science Foundation of China (NSFC); contract grant numbers: 50903072 and 10902099; contract grant sponsor: Zhejiang Province Natural Science Foundation; contract grant number: Y4100197; contract grant sponsor: Science Foundation of Zhejiang Sci-Tech University (ZSTU); contract grant number: 0901803-Y; contract grant sponsor: The Young Researchers Foundation of Key Laboratory of Advanced Textile Materials and Manufacturing Technology, Ministry of Education, Zhejiang Sci-Tech University; contract grant number: 2011QN02.
DOI 10.1002/pen.23358
Published online in Wiley Online Library (wileyonlinelibrary.com).

epigallocatechin (EGC), epicatechin gallate (ECG), and catechin gallate (EGCG). They have stimulated great interest due to their antimicrobial and antifungal properties and chelating of toxic heavy metals [22]. Previous studies have suggested that TP have functioned as both the "green" reductant and the capping agent for the synthesis of some metal nanospheres and no surfactant was used [23–26]. Inspired by their attractive properties, in this study, we chose TP as the green reducing agent to synthesize AgNPs.

In recent years, electrospinning technique has attracted great attention for it is the only method to produce fibers with nanosized diameter and high surface area [27, 28], and many kinds of the electrospun nanofibers have been chosen as the ideal support for nanoparticles [29–32]. PAN is an easy-electrospinning polymer, and more importantly, the C≡N groups on the surface of PAN nanofibers could be involved in the interaction with Ag ions through chelating effect, which may contribute to synthesize smaller AgNPs [33–36]. Consequently, we chose PAN to electrospun the nanofibers in the present work.

Herein, we proposed a convenient method of introducing TP as the green reductant to synthesize AgNPs through an in situ reduction approach in PAN/dimethyl formamide (DMF) solution. In the synthesis process, uniformly dispersed AgNPs with narrow size distributions in PAN nanofibers were obtained by electrospinning technique. The synthesized AgNPs/PAN nanofibers membranes showed good antibacterial activity against *E. coli* and *S. aureus*.

EXPERIMENTAL

Chemicals and Materials

DMF (99.5%) was obtained from Hangzhou Gaojing Fine Chemical. Silver nitrate ($AgNO_3$, 99.8%) was acquired from Changzhou Guoyu Environmental Technology. Polyacrylonitrile powder (PAN, $M_w \approx 1.4 \times 10^5$, $\rho = 1.14$–1.15 g cm^{-3}, copolymerized with 10 wt% methyl acrylate) was manufactured by Sinopec Shanghai Petrochemical. TP, with bulk density of 0.5 g cm^{-3}, was purchased from Xuancheng BaiCao Plant Industry and Trade, and the main chemical compositions are listed as follows: 12.5% EGC, 45.3% EGCG, 4.3% EC, and 9.1% ECG.

Synthesis of AgNPs in DMF Solution Using TP as the Reductant

The AgNPs were synthesized using TP as the reducing agent. $AgNO_3$ (0.068 g) was added to 45-ml DMF solution. The mixture was heated to 60°C and stirred by magnetic force vigorously, then 0.01 g of TP was dissolved in 5 ml DMF by sonicating for 1 min, and the TP/DMF solution was dropped to the mixture; at last, the mixture was kept uninterruptedly stirring for 60 min at 60°C. The AgNPs were also synthesized without TP as the reducing agent. $AgNO_3$ (0.069 g) was added to 50-mL DMF solution. The mixture was heated to 60°C and stirred by magnetic force vigorously for 60 min.

Synthesis of AgNPs in PAN/DMF Solution With and Without TP

The synthesis of AgNPs/PAN/DMF solution without extra reducing agent (DMF as the reductant) was carried out by the following procedure. The PAN solution was obtained by dissolving 6.371 g PAN powder into 45 ml DMF, stirring for 1 h at 60°C. $AgNO_3$ (0.159 g) powder was dissolved in 5 ml DMF at room temperature and added to the PAN/DMF solution dropwise within 2 min. Therefore, the mass fraction of PAN in the DMF solution was 12 wt% and the amount of $AgNO_3$ was 2.5 wt% (based on the weight of the PAN powder). The mixture was stirred for 60 min at 60°C.

The synthesis of AgNPs/PAN/DMF solution using TP as the reductant of $AgNO_3$ was similar as the above procedure. The only difference was that 0.012 g of TP was dissolved in 5-ml DMF solution and dropwise added to the system following on previous step. For contrast, another two samples with $AgNO_3$ content 1.0 and 7.5 wt% reduced by 0.005 and 0.036 g TP, respectively, were also prepared as the same procedure. All prepared samples were stored in liquid nitrogen.

Electrospinning of AgNPs/PAN Nanofibers

The above AgNPs/PAN/DMF solutions with $AgNO_3$ contents of 1.0, 2.5, and 7.5 wt% with reduction time of 60 min were fabricated into PAN nanofibers by electrospinning technique. The solutions were transferred into a syringe with a stainless copper needle at the tip and then electrospun under a fixed voltage of 12 kV and the needle to collector distance was 12 cm with the flow rate at 0.01 ml min^{-1}. The sie of syringe used for e-spinning was microinjection pump and the needle was + end. During e-spinning, the temperature was 25 ± 2°C and the humidity was 45%. The electrospun fibers were collected onto a piece of irrotational aluminum foil.

Characterization

Fourier Transform Infrared Spectroscopy. A thin layer of the prepared AgNPs/DMF/TP solution was spread on KBr pellets. The Fourier transform infrared spectroscopy (FTIR) analysis was conducted by a Nicolet 5700 FTIR spectrometer. The spectra were taken from 4000 to 400 cm^{-1} wavenumbers.

Ultraviolet–Visible Spectrascopy. The as-prepared AgNPs in the DMF and PAN/DMF solutions were examined by Lambda 900 Ultraviolet–visible spectrascopy (UV–vis) spectrophotometer (Perkin Elmer). The reference solution was DMF, and the spectra were collected over a wavelength range from 200 to 800 nm.

 DOI 10.1002/pen

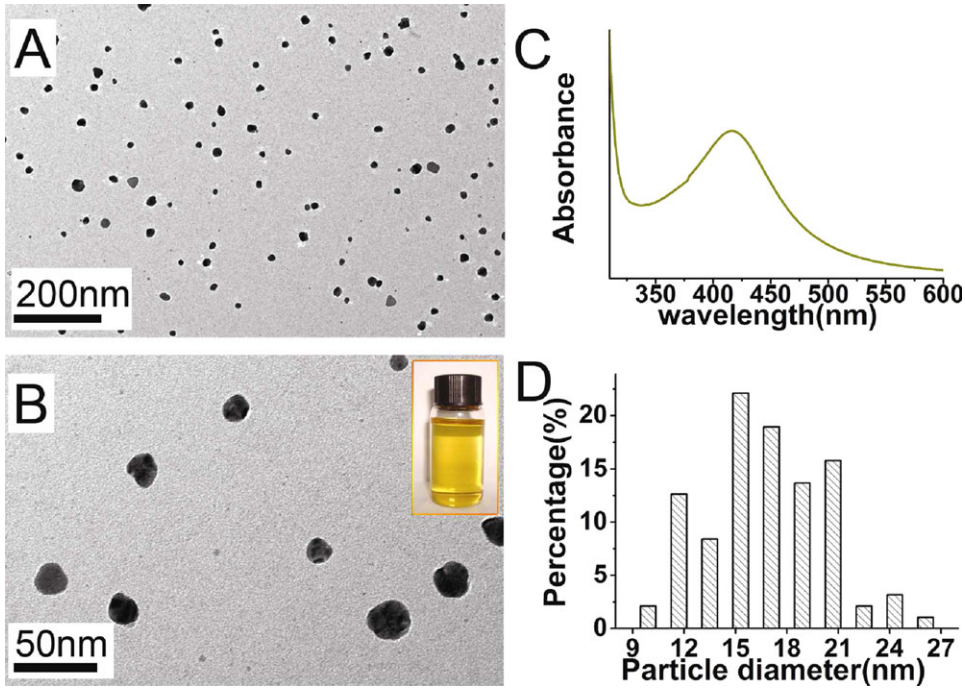

FIG. 1. TEM images of the AgNPs (A and B), particle diameter distribution, and UV–vis absorption spectrum of AgNPs. [Color figure can be viewed in the online issue, which is available at wileyonlinelibrary.com.]

Transmission Electron Microscopy and High-Resolution Transmission Electron Microscopy. The samples were prepared by dropping diluent AgNPs/DMF/TP solution onto a carbon-coated copper grid and dried under infrared lamp for 8 min. The AgNPs/PAN nanofibers samples were placed on ultrathin carbon-coated copper grids for observation. The images were acquired using JSM-2100 transmission electron microscope (JEOL, Japan) at an accelerating voltage of 200 kV.

Field-Emission Scanning Electron Microscopy (FE-SEM). The AgNPs/PAN nanofibers were plated with a thin layer of gold before observations. The morphology of electrospun AgNPs/PAN nanofibers were observed with a JSM-6700F field-emission scanning electron microscope (JEOL, Japan) under the voltage of 10.0 kV.

X-ray Photoelectron Spectroscopy. X-ray photoelectron spectra of pure PAN powder, TP, and AgNPs/PAN nanofibers were recorded by using an X-ray photoelectron spectrometer (Kratos Axis Ultra DLD) with an Aluminum (mono) K_α source (1486.6 eV). The high-resolution survey (pass energy = 48 eV) was performed at spectral regions relating to silver, oxygen, and nitrogen.

Antimicrobial Tests

The antibacterial activity of the AgNPs/PAN nanofiber membranes was assessed against bacterial strain Gram-negative bacteria *E. coli* ATCC 25922 and Gram-negative bacteria *S. aureus* ATCC 6538. For qualitative measurement of antibacterial activity, a modified agar diffusion assay (disc test) (ISO 20645: 2004, Textile fabrics–Determination of antibacterial activity–Agar diffusion plate test) was carried out. The inhibition zone was measured as activity against above two microbial species. For a typical procedure, the bacterial strains were inoculated in the sterilized Luria-Bertani (LB) medium and incubated overnight at 37°C with shaking before using. Then from each bacterial suspension, 200 μL volumes were withdrawn and spread uniformly over the agar plates. Small circular pieces of the AgNPs/PAN nanofiber membranes with the diameter of 2 cm were gently placed over the solidified agar gel in different petri dishes. Then the inoculated agars in the petri plates were kept for incubation at 37°C, after 18 h the lengths of inhibition zone were recorded.

RESULTS AND DISCUSSION

Synthesis of AgNPs Using TP as the Reductant

As observed in Fig. 1, AgNPs synthesized by using TP as the reductant in DMF solution with the reaction time of 60 min are obtained. Figure 1A and B reveals that most of the AgNPs are spherical and disperse uniformly, and the size distribution of the AgNPs is from about 10 to 26 nm. The inset in Fig. 1B shows that the prepared solution is transparent and the color is golden yellow. In addition, the intense absorption peak located at 416 nm in Fig. 1D is attributed to the surface plasma excitation of

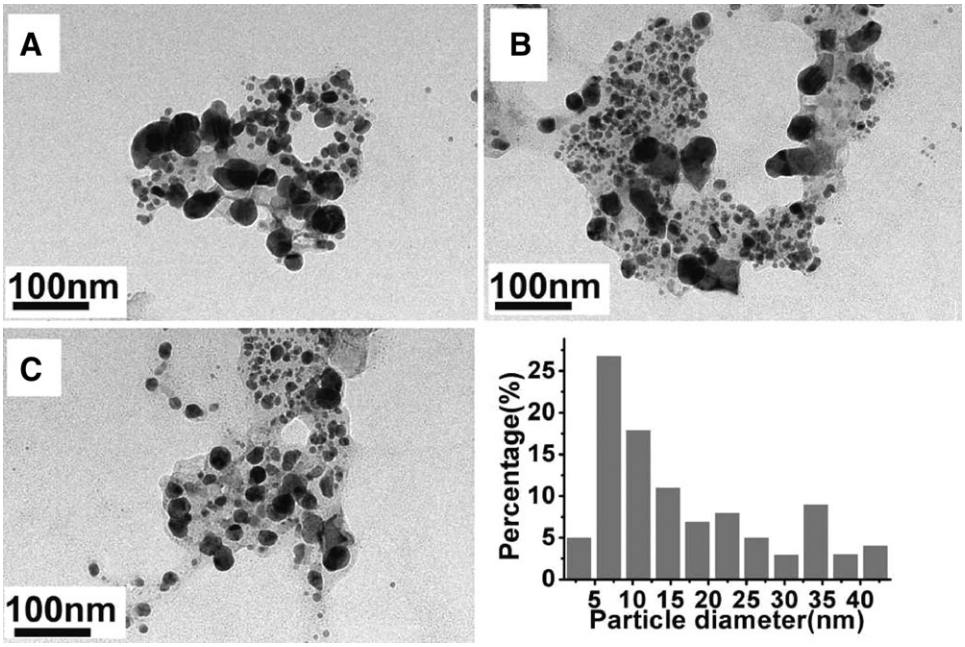

FIG. 2. TEM images of the AgNPs synthesized without TP and the corresponding size distribution.

AgNPs [37], so the UV–vis absorption spectrum of the prepared DMF solution can further confirm that the AgNPs were successfully synthesized.

Some previous studies have reported that the DMF also exhibits reducibility in the synthesis of AgNPs from $AgNO_3$ solution [38]. In the present work, the AgNPs synthesized using DMF as the reductant exhibit a relatively wide size distribution, and the average diameter is much bigger than that with the presence of TP (Fig. 2). Our previous work found that as consists of multiple hydroxyls, TP can chelate with the Ag ions and the chelated Ag ions can be reduced into Ag^0 atoms in situ, contributing to forming smaller and uniform AgNPs [39]. It is believed that the prepared AgNPs in the present approach were mainly reduced by TP, which will be discussed in the following work. The above data demonstrate that the green TP can serve as the reductant to synthesize AgNPs, suggesting a feasible procedure to produce AgNPs with narrow size distribution.

In the present approach, the supposed reaction between Ag ions and TP is illustrated in Fig. 3. FTIR analysis was used to testify the reducibility of TP toward Ag ions and investigate the chemical changes during the reaction process. The FTIR spectra of TP (A) and AgNPs/DMF/TP solution reacted for 60 min (B) are presented in Fig. 4. The broad absorption peak at 3361 cm^{-1} is assigned to the O—H stretching vibration of phenolic hydroxyls, suggesting the existence of hydrogen bonds in TP. The absorption band between 1550 and 1480 cm^{-1} is ascribed to the aromatic rings. The absorption peaks at 1455 and 1096 cm^{-1} are assigned to C—H alkanes in aromatic rings and C—O stretching vibration, respectively. The typical absorption peaks of DMF can be assigned as follows: 2928 and 2860 cm^{-1} (C—H stretching vibration), 1387 cm^{-1} (C—H in-plane vibration), 1676 cm^{-1} (C=O stretching vibration), and 660 cm^{-1} (N—C=O flexural vibration). However, an obvious change is observed in the wide hydroxyl band 2820–3687 cm^{-1} region for curve b. The absorption peak at 3361 cm^{-1} gets relatively narrow and shifts to 3530 cm^{-1}, and it indicates that part of hydroxyls in TP participate in the redox reaction between TP and Ag ions. Furthermore, the peaks at 1344, 1147, and 1037 cm^{-1} ascribed to C—O—H stretching vibration, O—H damping vibration and C—O—H stretching vibration of phenolic hydroxyls in TP are nearly vanished, implying the involvement of the O—H groups in the reduction of Ag ions. Additionally, the peak at 1101 cm^{-1} in Fig. 4B is much stronger than that in Fig. 4A, and it is mainly attributed to the oxidization of part of aldehyde groups in DMF to carboxyl groups.

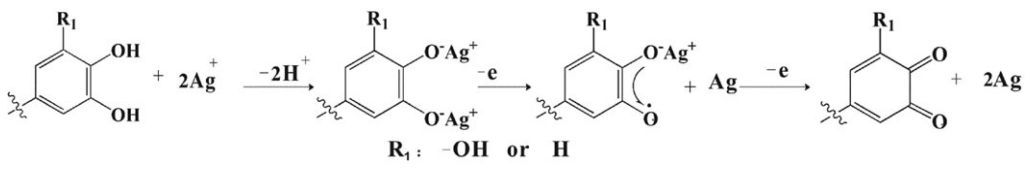

FIG. 3. Illustration of the reaction between Ag ions and TP.

 DOI 10.1002/pen

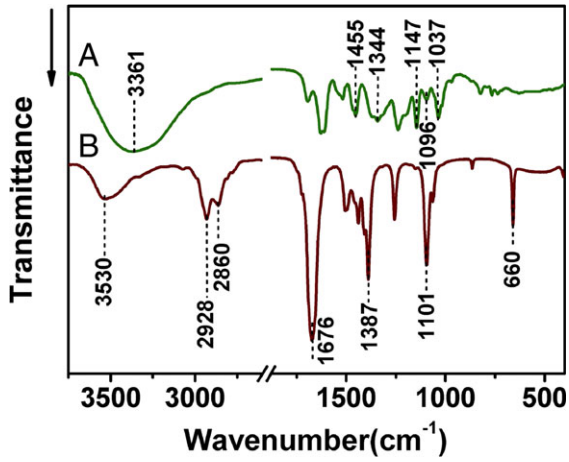

FIG. 4. The FTIR spectra of TP (A) and AgNPs/DMF/TP solution (B). [Color figure can be viewed in the online issue, which is available at wileyonlinelibrary.com.]

Fabrication of Electrospun PAN Nanofibers with AgNPs

In the above work, we successfully synthesized the well-dispersed AgNPs using TP as the effective reductant in DMF solution. Then, we propose a facile route to fabricate AgNPs/PAN nanofibers by combining the electrospinning technique and an in situ reduction approach. In the present investigations, we fabricated electrospun PAN nanofibers with uniformly dispersed AgNPs, which are shown in Fig. 5. From the figure, it can be seen that the AgNPs in PAN nanofibers exhibit very small diameter and narrow size distribution. With the increasing concentration of $AgNO_3$, the amount of the AgNPs in PAN nanofibers increases gradually. As shown in the diameter distribution histogram, the average particle diameters of AgNPs in PAN nanofibers are about 2.8, 5.3, and 4.5 nm, corresponding to the $AgNO_3$ mass fractions of 1.0, 2.5, and 7.5 wt%, respectively. The size of AgNPs shown in Fig. 5B and C is much bigger than that in Fig. 5A, which may result from the different concentration of $AgNO_3$ and TP [37]. Surprisingly, in contrast to the AgNPs synthesized in DMF solution, as shown in Fig. 1, the AgNPs obtained by in situ approach in PAN nanofibers possess much smaller diameter, which indicates that the PAN polymer may act as a particular stabilizer and prevent the particle growth in the process of synthesis of AgNPs, and it will be discussed later. The high-resolution transmission electron microscopy (HRTEM) image of AgNPs is shown in Fig. 6. The AgNPs possess a well-resolved lattice planes, and the interplanar spacing is about 0.243 nm, corresponding to the (111) planes of fcc Ag.

In the present investigations, DMF was utilized as the solvent of PAN for electrospinning. However, DMF also can be used as a reductant for Ag ions; therefore, we compared the reducibility of DMF and TP by reducing $AgNO_3$ in PAN/DMF solutions. The UV–vis spectra, including $AgNO_3$/PAN/DMF solution reduced with and without TP, are shown in Fig. 7. Each curve has a typical and narrow absorption peak around 275 nm, which corresponds to AgNPs clusters or small AgNPs because of the interband transitions [40, 41]. With the increase of reac-

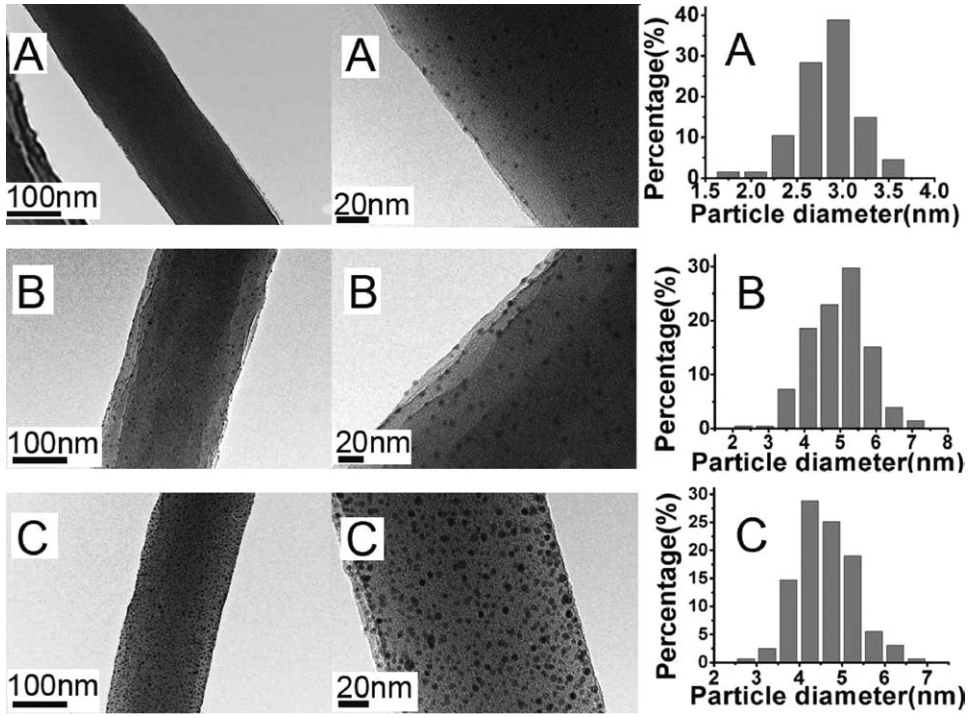

FIG. 5. TEM images of AgNPs/PAN nanofibers: (A) 1.0 wt%; (B) 2.5 wt%; (C) 7.5 wt%, with the corresponding diameter distribution histogram of the immobilized AgNPs.

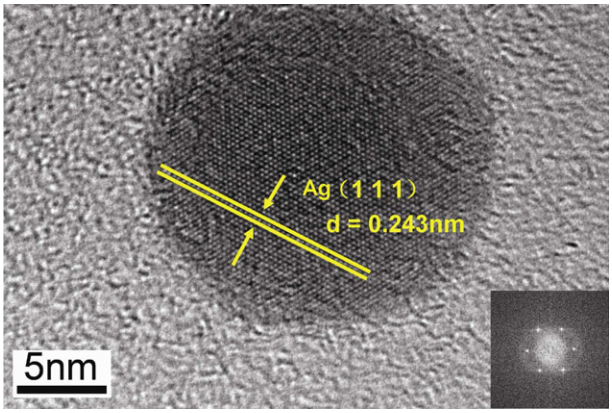

FIG. 6. HRTEM image of the AgNPs. [Color figure can be viewed in the online issue, which is available at wileyonlinelibrary.com.]

tion time from 1, 15, 30, and 45 to 60 min in both Fig. 7A and B, the absorption peaks exhibit redshifts from 277 to 281 nm. From Fig. 7A, it can be seen that the absorption peak around 275 nm become more intense with the increase of reaction time, indicating the reduction activity of DMF for Ag ions. However, with the addition of TP, the absorption of AgNPs appears much stronger even within very short reaction time, which indicates that TP display much higher reductive activity in terms of reducing Ag ions. With the introduction of TP as the reductant, the intensity of the absorption peak of AgNPs increase with reaction time going on, as shown in Fig. 7B. The inset photo portrays the color changes from colorless to yellow gradually. Typically, the intensive surface plasma resonance (SPR) band of AgNPs has a hypsochromic shift from 415 to 386 nm, and it is attributed to the free

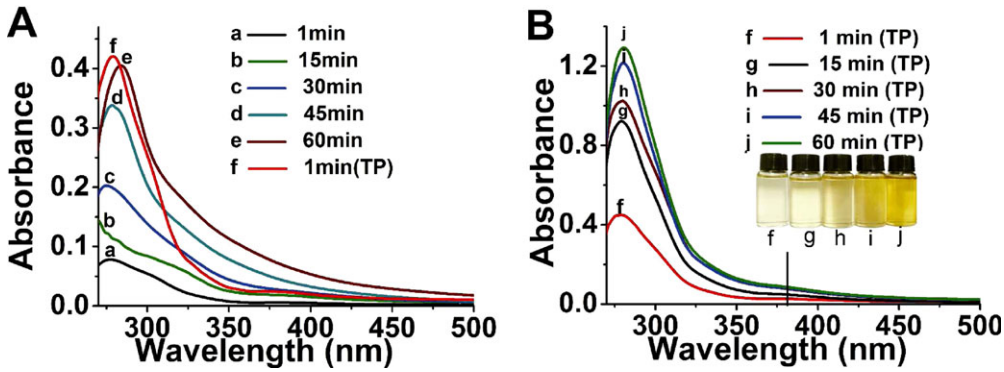

FIG. 7. UV–vis spectra of $AgNO_3$ (2.5 wt%)/DMF solution in the presence of PAN (12 wt%) with and without TP. [Color figure can be viewed in the online issue, which is available at wileyonlinelibrary.com.]

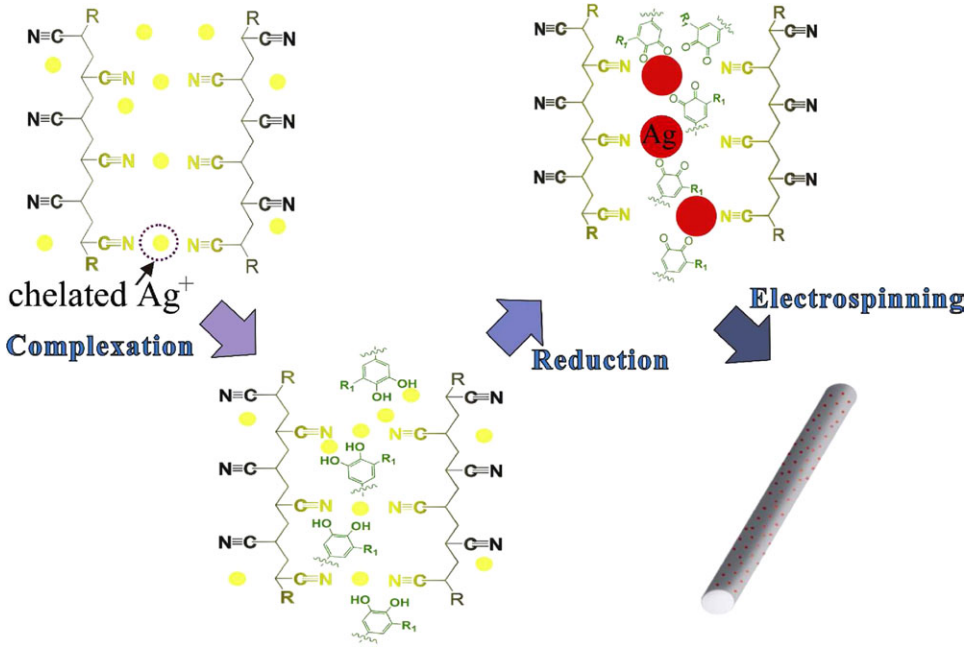

FIG. 8. Fabrication procedure of AgNPs immobilized in PAN nanofibers. [Color figure can be viewed in the online issue, which is available at wileyonlinelibrary.com.]

 DOI 10.1002/pen

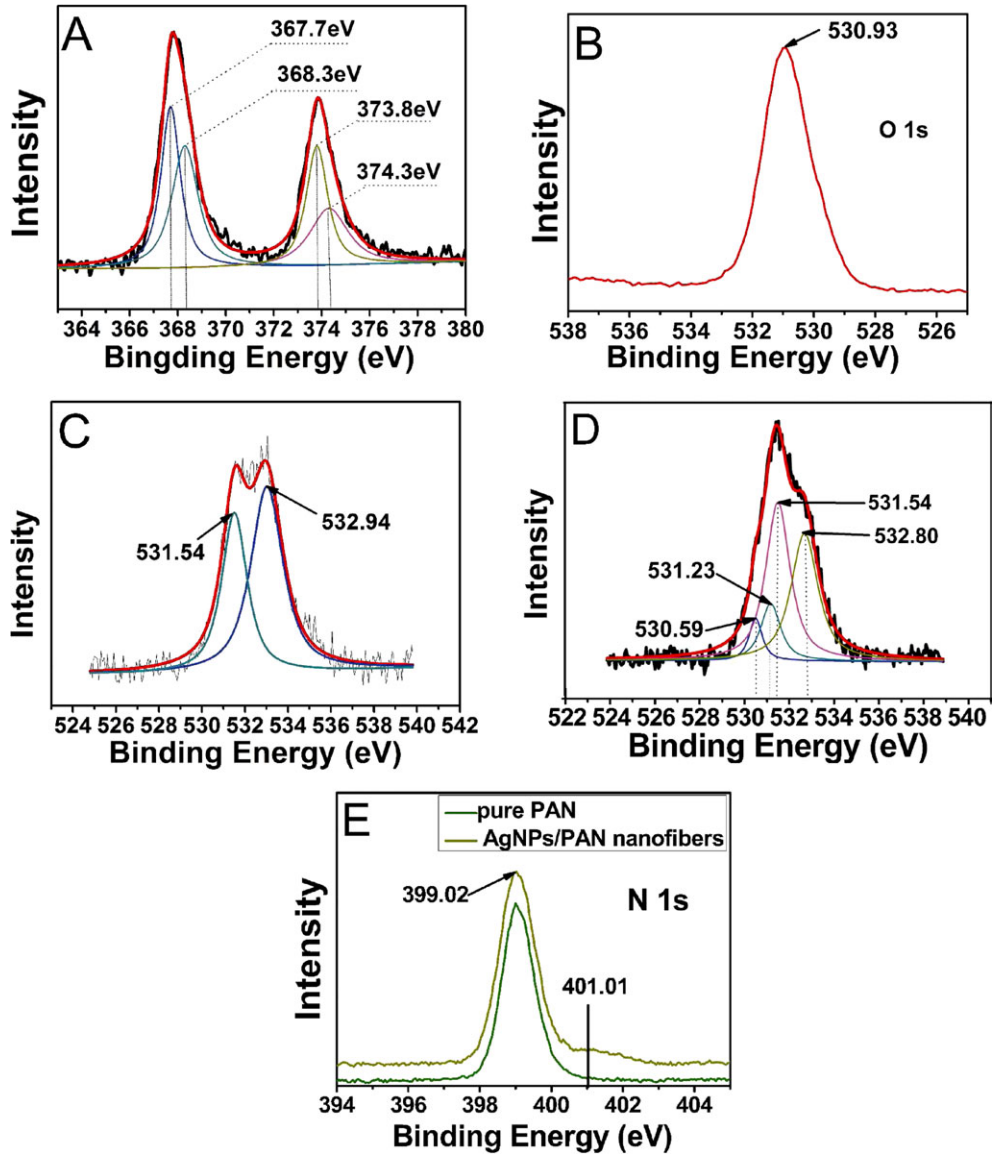

FIG. 9. XPS spectra of Ag, oxygen, and nitrogen atoms. (A) Ag 3d of AgNPs/PAN nanofibers; (B) O 1s of TP; (C) O 1s of the pure PAN; (D) O 1s of AgNPs/PAN nanofibers. (E) N 1s in pure PAN powder and AgNPs/PAN nanofibers. [Color figure can be viewed in the online issue, which is available at wileyonlinelibrary.com.]

conduction electrons on the surface of AgNPs (intraband excitation) [41]. And, the absorption strength appears relatively weak is due to the cyano group which is an effective extinction reagent.

Figure 8 summarized procedures for the typical preparation of AgNPs/PAN nanofibers. It is supposed that chelating effects of Ag ions and Ag nucleus with cyano groups in PAN polymer and phenolic hydroxyls in TP molecules play a crucial role in the synthesis of AgNPs in PAN nanofibers, which will be proved by X-ray photoelectron spectroscopy (XPS) results and discussed later. In the present procedure, the PAN polymer possesses a large amount of cyano groups, which can "anchor" Ag ions in the PAN/DMF solution through chelating effect. The addition of TP, introducing multiple phenolic hydroxyls to the reaction system, results in an increasing binding sites for Ag ions through chelating effect between Ag ions and the phenolic hydroxyls of TP molecules. The high density of functional groups (phenolic hydroxyls) in TP will reduce Ag ions to metallic Ag to form Ag nucleus accompanying the oxidation of phenolic hydroxyls to quinones. Then other Ag ions will gradually be reduced by TP and grow on the surface of the formed Ag nucleus. Because of the high viscosity of the solution and the chelating effect between Ag nucleus and phenolic hydroxyls in TP molecules, the Ag nucleus cannot easily collide with each other to coagulate. In addition, due to the chelating effects between cyano groups and Ag ions, the rate of Ag crystal growth is restrained, consequently, causing relatively smaller AgNPs compared with those

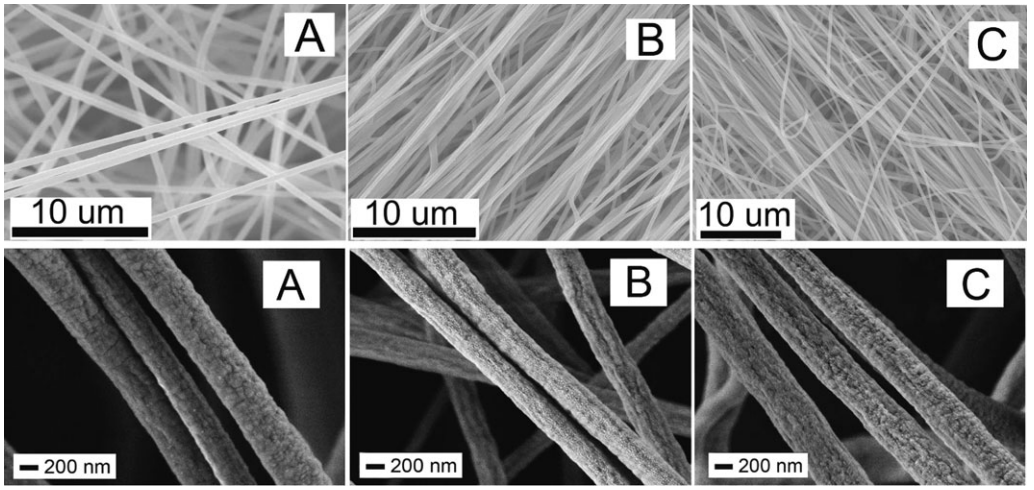

FIG. 10. SEM images of electrospun nanofibers with different concentration of $AgNO_3$. (A) 1.0 wt%; (B) 2.5 wt%; (C) 7.5 wt%.

synthesized in DMF solution. At the same time, the formed quinones and free hydroxyls are able to stabilize AgNPs by interaction with the surface Ag atoms through electron donation and acceptation interaction, promoting the formation of spherical AgNPs with smaller sizes [6, 26]. The strong interactions between the reduced AgNPs and the functional groups from aromatic TP and PAN guarantee the good dispersion of the synthesized AgNPs in the electrospun PAN nanofibers. Overall, the PAN polymer act as a chelating agent and the TP serve as both the reductant and the protective agent, which plays a crucial role in preventing the particle growing to obtained smaller AgNPs.

To verify the above procedure and the chelating effects of Ag ions and Ag nucleus with cyano groups and phenolic hydroxyls, XPS characterization on Ag, oxygen, and nitrogen atoms in AgNPs/PAN nanofibers, pure PAN and TP were performed, and the results are shown in Fig. 9. As shown in Fig. 9A, a pair of doublets is observed in the Ag 3d region of AgNPs/PAN nanofibers, which is attributed to the spin–orbital splitting of $3d_{5/2}$ and $3d_{3/2}$ in Ag 3d core level, indicating the two kinds of chemical environments in the synthesized AgNPs. Compared with Ag^0, the two peaks located at 368.3 and 374.3 eV are assigned to the Ag atoms of AgNPs [42], whereas two other new peaks located at 367.7 and 373.8 eV are observed, it is resulted from the chelating effects of Ag with cyano groups and phenolic hydroxyls [25, 43, 44]. The chelating effects of Ag with cyano groups and phenolic hydroxyls will induce an image dipole on the Ag atoms' surface, consequently a part of positive charges from the surface of AgNPs are donated to the stabilizer, causing a negative shift in Ag 3d core level.

The XPS spectra of oxygen for pure PAN and TP are shown in Fig. 9B and C, respectively. For pure PAN, the peaks at 531.54 and 532.94 eV are assigned to the two types of oxygen atoms in the methyl acrylate copolymerized with acrylonitrile. There is only one peak at 530.93 eV in O 1s signal from TP, which is mainly attributed to C—OH in phenolichydroxyl. For AgNPs/PAN nanofibers, as shown in Fig. 9D, the O 1s signal peak can be divided into four peaks. Two peaks at 531.54 and 532.80 eV are accorded with that of pure PAN O 1s. As discussed above, after reaction with Ag ions, the O 1s peak corresponding to C—OH in TP is changed, oxidized from phenolic hydroxyls to quinones. Therefore, there is a shift of about 0.3 eV, from 531.23 to 530.93 eV, for the O 1s in TP. In addition, a new peak arises at 530.59 eV, attributing to the quinones from the oxidization of TP. In Fig. 9E, the peak located at 399.02 eV standing for N 1s is from cyano groups of PAN. However, another small peak arises at 401.01 eV, which may be attributed to the chelating interactions between nitrogen and Ag.

As discussed above, due to the chelating interactions of Ag ions with cyano groups and phenolic hydroxyls, PAN polymer and TP both serve as stabilizer during the synthesis of AgNPs in PAN nanofibers, preventing AgNPs from aggregation and obtaining AgNPs with relatively small size and uniform dispersion in PAN nanofibers.

Antibacterial Activity

Figure 10 shows the SEM images of electrospun nanofibers with different mass fraction of $AgNO_3$. The majority diameter of the individual fibers obtained from these solutions is about 200–300 nm, which is identical with the values observed by transmission electron microscopy (TEM). Figure 11 shows the typical results of the antibacterial tests for the purpose of a qualitative evaluation. The lengths of the inhibition zones of the AgNPs/PAN nanofiber membranes were measured. It is observed from Fig. 11 that the pure PAN nanofiber membranes show nonbac-

 DOI 10.1002/pen

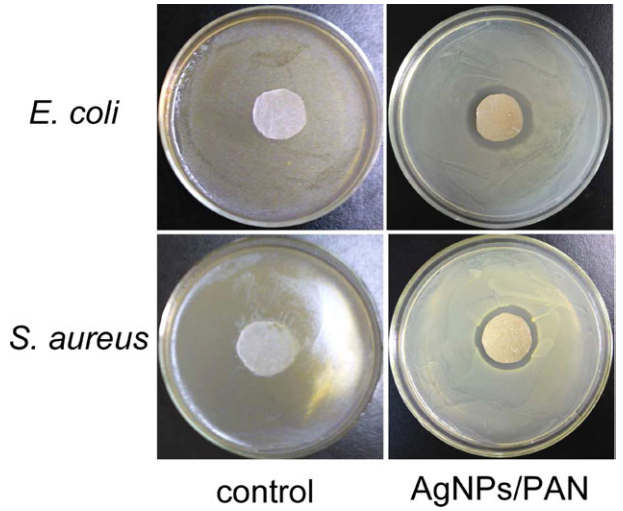

FIG. 11. Pictures of inhibition zone test of AgNPs/PAN nanofiber membranes with 7.5 wt% (based on the weight of PAN powder) concentration of $AgNO_3$. [Color figure can be viewed in the online issue, which is available at wileyonlinelibrary.com.]

terial properties against either *E. coli* or *S. aureus* bacteria. However, the antibacterial activity of the AgNPs/PAN nanofiber membranes against both *E. coli* and *S. aureus* bacteria is proved by zones of bacterial growth inhibition around the circular pieces, and the lengths of inhibition zones are both about 5 mm, which indicates the good antibacterial property of AgNPs/PAN nanofiber membranes. In addition, as shown in Fig. 10, magnified images of electrospun AgNPs/PAN nanofibers exhibit relative rough surface, it is supposed that the synthesized AgNPs in PAN nanofibers possess potential and promising applications in antibacterial and catalytic areas.

CONCLUSIONS

AgNPs with uniform dispersion in PAN nanofibers were successfully synthesized using TP as the reductant and the stabilizer. The reducibility of TP was confirmed by UV–vis and FTIR. TEM results suggested that the spherical AgNPs with diameter about 5 nm were immobilized on the surface and in the interior of PAN nanofibers by electrospinning technology. The amount of AgNPs in nanofibers increased gradually with the increasing of $AgNO_3$ concentration in the original reaction system. The interactions of Ag with PAN and TP were investigated by XPS and the results suggested that PAN polymer and TP both served as stabilizer during the synthesis of AgNPs in PAN nanofibers, because of the chelating interactions of Ag with cyano groups and phenolic hydroxyls. The prepared AgNPs/PAN nanofiber membranes exhibited good antibacterial activity against *E. coli* and *S. aureus*. The synthesized AgNPs in PAN nanofibers exhibit good antibacterial property and may be used for antibacterial and catalytic applications.

REFERENCES

1. R.D. Jean, K.C. Chiu, T.H. Chen, C.H. Chen, and D.M. Liu, *J. Phys. Chem. C*., **114**, 37 (2010).
2. S. Anandhakumar, S.P. Vijayalakshmi, G. Jagadeesh, and A.M. Raichur, *ACS Appl. Mater. Interfaces*, **3**, 9 (2011).
3. A. Serra, E. Filippo, M. Re, M. Palmisano, V.M. Antisari, A. Buccolieri, and D. Manno, *Nanotechnology*, **20**, 16 (2009).
4. P. Christopher and S. Linic, *J. Am. Chem. Soc*., **130**, 34 (2008).
5. S.L. Shen, J. Zhuang, Y. Yang, and X. Wang, *Nanoscale*, **3**, 1 (2011).
6. J.L. Guo, H. Wu, X.P. Liao, and B.J. Shi, *Phys. Chem. C*., **115**, 48 (2011).
7. C.L. Du, Y.M. You, X.J. Zhang, K. Johnson, and Z.X. Shen, *Plasmonics*, **4**, 3 (2009).
8. U.K. Parashar, V. Kumar, T. Bera, P.S. Saxena, G. Nath, S.K. Srivastava, and R. Giri, *Nanotechnology*, **22**, 41 (2011).
9. R. Nirmala, F.A. Sheikh, M.A. Kanjwal, J.H. Lee, S.J. Park, R. Navamathavan, and H.Y.J Kim, *Nanopart. Res*., **13**, 5 (2011).
10. E. Falletta, M. Bonini, E. Fratini, A.L. Nostro, G. Pesavento, A. Becheri, P.L. Nostro, P. Canton, and P. Baglioni, *J. Phys. Chem. C*., **112**, 31 (2008).
11. F.M. Kelly and J.H. Johnston, *ACS Appl. Mater. Interfaces*, **3**, 4 (2011).
12. C. Zhao, G.P. Jin, L.L. Chen, and B. Yu, *Food Chem*., **129**, 2 (2011).
13. S.H. Jeon, P. Xu, B. Zhang, N.H. Mack, H. Tsai, L.Y. Chiang, and H. Wang, *J. Mater. Chem*., **21**, 8 (2011).
14. S. Porel, N. Venkatram, D.N. Rao, and T.P. Radhakrishnan, *J. Nanosci. Nanotechnol*., **7**, 6 (2007).
15. B.S. Fu, M.N. Missaghi, C.M. Downing, M.C. Kung, H.H. Kung, and G.M. Xiao, *Chem. Mater*., **22**, 7 (2010).
16. P.K. Rastogi, V. Ganesan, and S. Krishnamoorthi, *Mater. Sci. Eng., B*, **177**, 6 (2012).
17. S.K. Srivastava and M. Constanti, *J. Nanopart. Res*., **14**, 831 (2012).
18. P. Raveendran, J. Fu, and S.L. Wallen, *Green Chem*., **8**, 1 (2006).
19. T.H. Tsai, S. Thiagarajan, and S.M. Chen., *Electroanalysis*, **22**, 6 (2010).
20. Y.S. Lin, S.S. Wu, and J.K. Lin, *J. Agric. Food Chem*., **51**, 4 (2003).
21. M. Daglia, A. Papetti, P. Grisoli, and C.J. Aceti, *Agric. Food Chem*., **55**, 13 (2007).
22. C. Anesini, G.E. Ferraro, and R.J. Filip, *Agric. Food Chem*., **56**, 19 (2008).
23. Y.N. Chen, Y.D. Lee, H. Vedala, B.L. Allen, and A. Star, *ACS Nano*., **4**, 11 (2010).
24. Y. Wang, Z.X. Shi, and J. Yin, *ACS Appl. Mater. Interfaces*., **3**, 4 (2011).
25. H. Wu, X. Huang, M.M. Gao, X.P. Liao, and B. Shi, *Green Chem*., **13**, 3 (2011).

26. X. Huang, H. Wu, X.P. Liao, and B. Shi, *Green Chem*., **12**, 3 (2010).
27. S.Y. Wei, J. Sampathi, Z.H. Guo, N. Anumandla, D. Rutman, A. Kucknoor, L. James, and A. Wang, *Polymer*, **52**, 25 (2011).
28. Y.L. Huang, A. Baji, H.W. Tien, Y.K. Yang, S.Y. Yang, C.C. Ma, H.Y. Liu, Y.W. Mai, and N.H. Wang, *Nanotechnology*, **22**, 47 (2011).
29. E. Formo, M.S. Yavuz, E.P. Lee, L. Lane, and Y.N. Xia, *J. Mater. Chem*., **19**, 23 (2009).
30. G.M. Kim, A. Wutzler, H.J. Radusch, G.H. Michler, P. Simon, R.A. Sperling, and W.J. Parak, *Chem. Mater*., **17**, 20 (2005).
31. P.O. Rujitanaroj, N. Pimpha, and P. Supaphol, *Polymer*, **49**, 21 (2008).
32. X. Fang, H. Ma, S. Xiao, M.W. Shen, R. Guo, X.Y. Cao, and X.Y. Shi, *J. Mater. Chem*., **21**, 12 (2011).
33. X.G. Li, R. Liu, and M.R. Huang, *Chem. Mater*., **17**, 22 (2005).
34. X.G. Li, X.L. Ma, J. Sun, and M.R. Huang, *Langmuir*, **25**, 3 (2009).
35. X.G. Li, H. Feng, and M.R. Huang, *Chem. Eur. J*., **16**, 33 (2010).
36. X.G. Li, M.R. Huang, and S.X. Li, *Acta Mater*., **52**, 18 (2004).
37. M.C. Moulton, L.K. Braydich-Stolle, M.N. Nadagouda, S. Kunzelman, S.M. Hussain, and R.S. Varma, *Nanoscale*, **43**, 6 (2010).
38. I. Pastoriza-Santos and L.M. Liz-Marzan, *Adv. Funct. Mater*., **19**, 5 (2009).
39. H. Zhu, M.L. Du, M.L. Zou, C.S. Xu, N. Li, and YaQin Fu, *J. Mater. Chem*., **22**, 18 (2012).
40. S. Pocovi-Martinez, M. Parreno-Romero, S. Agouram, and J. Perez-Prieto, *Langmuir*, **27**, 9 (2011).
41. K. Akhbari and A. Morsali, *Crystal Growth Design*., **7**, 10 (2007).
42. J. Zhang, Y. Yuan, X.W. Xu, X.L. Wang, and X.R. Yang, *ACS Appl. Mater. Interfaces*, **3**, 10 (2011).
43. L.H. Jia, S. Zhang, F.N. Gu, Y. Ping, X.F. Guo, Z.Y. Zhong, and F.B. Su, *Micropor Mesopor Mat*., **149**, 1 (2012).
44. X.Y. Yang, A. Wolcott, G. Wang, A. Sobo, R.C. Fitzmorris, F. Qian, J.Z. Zhang, and Y. Li, *Nano Lett*., **9**, 6 (2009).

 DOI 10.1002/pen